https://icbem-icebi-eit-2022.org/

International Conference on Bioelectromagnetism,
Electrical Bioimpedance, and Electrical Impedance Tomography

ICBEM-ICEBI-EIT 2022

June 29 – July 1, 2022
Virtual / Kyung Hee University

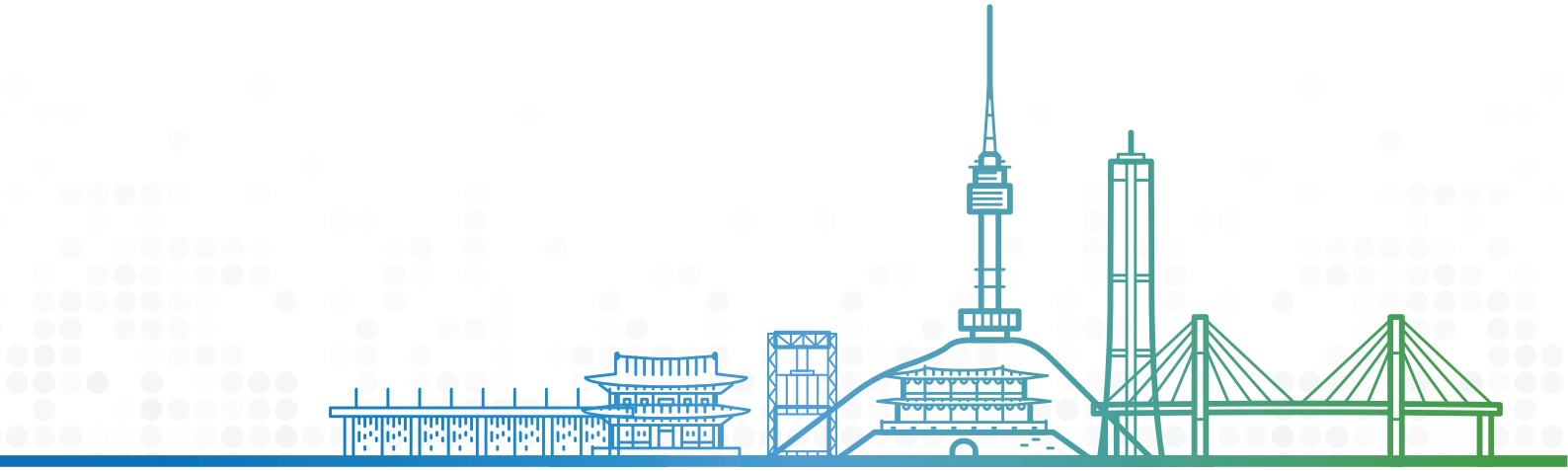

Hosted by ICBEM Bioelectromagnetism, ICEBI Electrical Bioimpedance, EIT Electrical Impedance Tomography

Supported by IFMBE

Organized by KYUNG HEE UNIVERSITY, Impedance Imaging Research Center

Sponsored by BiLab, scio spec, Dräger, Ikju Electronics, KOREA TOURISM ORGANIZATION

Proceedings of the International Conference of Bioelectromagnetism, Electrical Bioimpedance, and Electrical Impedance Tomography June 29 – July 1, 2022 / Kyung Hee University, Seoul, Korea

Assessment of electroporation in different complex structures by means of MREIT

Marko Stručić[1], Jessica Genovese[2], Vitalij Novickij[3], Samo Mahnič-Kalamiza[1], Igor Serša[4], Damijan Miklavčič[1] and Matej Kranjc[1]

[1] University of Ljubljana, Faculty of Electrical Engineering, Tržaška c. 25, 1000 Ljubljana, Slovenia
[2] University of Bologna, Department of Agricultural and Food Sciences, P. Goidanich 60, Cesena, Italy
[3] Institute of High Magnetic Fields, Vilnius Gediminas Technical University, Naugarduko g. 41, 03227 Vilnius, Lithuania
[4] Institut "Jožef Stefan", Jamova cesta 39, 1000 Ljubljana, Slovenia

Correspondence : Matej Kranjc, e-mail : matej.kranjc@fe.uni-lj.si

Abstract- The aim of our study was to investigate the degree of membrane permeabilisation by applying Pulsed Electric Field (PEF) treatment to plant and animal food matrices (potato, apple, chicken) using magnetic resonance electrical impedance tomography and T_2 mapping. The effect of electroporation treatment on T_2 relaxation times was evaluated by comparing the electric field distribution obtained by magnetic resonance electrical impedance tomography with the induced decrease of T_2 values. The research results provided useful insights into the evaluation of electroporation and suggest that magnetic resonance electrical impedance tomography could be used as an efficient tool to improve the efficacy of electroporation treatments.

Keywords: electroporation, PEF treatment, electric field, magnetic resonance imaging, magnetic resonance electrical impedance tomography.

1. Introduction

Electroporation or Pulsed Electric Field (PEF) treatment of food is an emerging industrial processing technology with a potential to replace conventional thermal food processes widely used to improve food stability and guarantee its microbiological safety [1]. This technology uses application of short electric pulses with high amplitude affecting cell membrane permeability or in extreme cases even destroying the cell membrane. PEF treatment requires moderate energy consumption, is fast, allows for better retention of flavour and colour, and preserves nutritional properties of foods [2]. Despite the numerous benefits of PEF treatment, there is still debate about the appropriate assessment of its effects. In this respect, several research papers reported on the analysis of the electric current signals during the application of the high-voltage pulse, demonstrating that the dynamics of electric current can be used as a key characterization feature of tissue electroporation [3,4]. However, there are limits in obtaining detailed information regarding the detection and quantification of electroporation effects in highly inhomogeneous multicellular systems, with a clear drawback of these results being affected by additional phenomena, which can be superimposed or altered in other ways. Magnetic resonance electric impedance tomography (MREIT) is a method capable of reconstructing the electric field distribution during pulse delivery indirectly through use of magnetic resonance imaging (MRI) and numerical algorithms, thus making it an attractive tool for monitoring and evaluation of electroporation treatment of tissues.

The goal of our investigation was to explore the level of membrane permeabilization in plant and animal tissues as an underlying mechanism of PEF treatment from subjecting these tissues to PEF treatment, whereby we employed different MRI assessment methods (current density imaging, MREIT, and transversal relaxation time T_2 mapping). Experiments were performed in apple fruit and potato tuber tissue, since these vegetable matrices are increasing in complexity and of substantial interest in industrial PEF applications. Additionally, chicken broiler *Pectroalis major* muscle was selected as a reference skeletal muscle due to its high homogeneity, as it is almost completely composed of IIB (fast twitch glycolytic) type fibres [5].

2. Materials and Methods

2.1 Plant and Animal Tissues

The apples (*Malus domestica*, cv 'Golden Delicious') and potatoes (*Solanum tuberosum*, cv 'Liberta') used for this study were purchased at the local market (Ljubljana, Slovenia). Boneless and skinless *Pectoralis major* muscles were obtained from the same flock of broiler chickens (Ross 308 hybrid, slaughter age 46 days, average weight 2.9 kg) farmed and processed under commercial conditions and, before trials, stored at 1 °C. Each fillet was sampled using the cranial portion of the breast and cut along the direction of muscle fibres. From each sample, disks 26 mm in diameter and 30 mm in thickness were manually cut using a sharp stainless steel cork-borer.

2.2 Pulsed Electric Field Treatment

Electroporation treatment of the cylindrical-shape plant samples was performed using an electric pulse generator lab prototype (Novickij et al., 2016) connected to a pair of custom-built needle electrodes inserted into the sample tissue. The electrodes, made of platinum/iridium alloy (Pt/Ir: 90/10 %), had a diameter of 1 mm and were placed at a centre-to-centre distance of 10.4 mm. PEF protocol consisted of two sequences of 4 pulses with a duration of 100 µs per pulse and with a repetition rate of 5000 s^{-1}. For every tissue studied, the voltage amplitude was adjusted to obtain a sufficient signal-to-noise ratio of the electric field in the sample (i.e. apple 1180 V; potato 750 V; chicken 860 V). The trigger input of the generator was connected to the MRI spectrometer and synchronized with the Current Density Imaging (CDI) pulse sequence. The delivery of the electric pulses was monitored with an oscilloscope (WavePro 7300A, LeCroy, NY, USA) and a current probe (AP015, LeCroy, NY, USA).

2.3 Current Density Imaging and Magnetic Resonance Electrical Impedance Tomography

Magnetic Resonance Imaging (MRI) was performed on tissues while applying PEF treatment, following the method described in [6]. The MRI scanner consisted of a 2.35 T horizontal bore superconducting magnet (100 MHz proton MR frequency) (Oxford Instruments, Abingdon, UK) connected to an Apollo spectrometer (Tecmag, Houston TX, USA) and equipped with microimaging accessories with maximum gradients of 250 mT/m (Bruker, Ettlinger, Germany). The samples were scanned during the application of the electrical pulses using the Current Density Imaging (CDI) method to obtain a map of the current-induced magnetic field change in the sample, as determined by MRI phase shift registration [7]. The map was then processed using the J-substitution algorithm of the magnetic resonance electrical impedance tomography (MREIT), which is based on the iterative solution of the Laplace's equation [8]. The CDI data, together with the known sample geometry and the potentials at the electrodes, were used as inputs to the MREIT algorithm to calculate the map of distribution of the electric field in the plant tissue. In this study, the CDI pulse sequence (Fig. 1) was performed with two acquisitions of relaxation enhancement (RARE) imaging sequence [9] using the following parameters: field of view 30 mm, imaging matrix 64 x 64, inter-echo delay 2.64 ms, and slice thickness of 8 mm. In the sequence, electric pulses were delivered between the excitation RF pulse and the first refocusing RF pulse. The MREIT algorithm was solved using the finite element method with the MATLAB 2021b numerical computing environment (MathWorks, Natick, MA, USA) on a desktop PC.

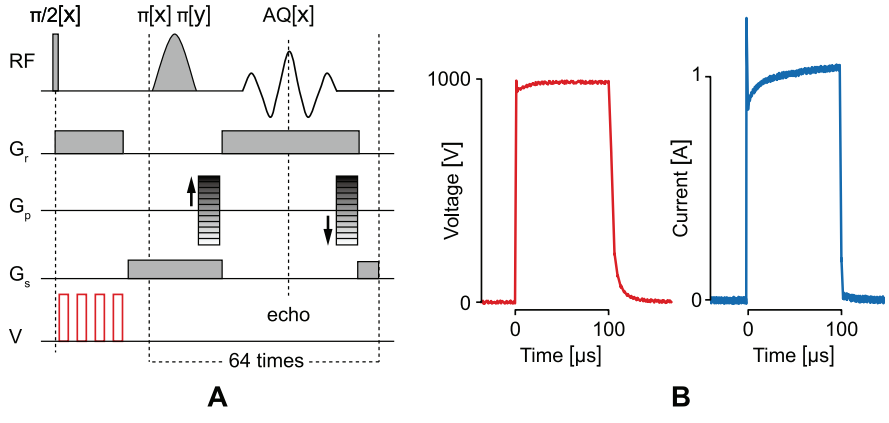

Figure 1. (A) Two-shot RARE CDI sequence that was used to create a map of current-induced magnetic field changes. The first part of the sequence is a current encoding part with four (100 µs long) high-voltage electric pulses (red line) delivered immediately after the nonselective 90° radiofrequency (RF) excitation pulse. (B) Measurements of the voltage (red line) and electric current (blue line) of one of the representative electric pulses.

2.4 T_2-weighted imaging

Plant tissues were dynamically monitored with a multiparametric MRI consisting of T_2-weighted imaging. A multi-spin-echo (MSE) imaging sequence based on the Carr-Purcell-Meiboom-Gill (CPMG) multi-echo train (Carr and Purcell, 1954) was chosen to acquire T_2-weighted MR images before and immediately after PEF treatment (i.e. a total of 18 min after pulsation). The T_2 pulse sequence was performed with the following imaging parameters: field of view 30 mm;

imaging matrix 128 x 128; inter-echo delay 70 ms, slice thickness of 5.1 mm. T_2 maps were calculated using the MRI Analysis Calculator plug-in of ImageJ image processing software (NIH, US), fitting raw MSME data to variable TE (n = 8 echoes) ($R^2 > 0.9$). Additional analysis and quantitative assessment of the T_2-weighted images was performed using MATLAB 2021b (MathWorks, Natick, MA, USA) on a desktop PC.

3. Results

In our study, we obtained the distributions of electric fields in apple, potato and chicken samples subjected to PEF treatment. In addition to the MREIT, T_2 mapping was also performed in the same samples to determine the changes in tissue water content that would occur due to electroporation. The effect of electroporation treatment on T_2 relaxation times was evaluated by measuring T_2 times before and after treatment. In addition, the changes in T_2 relaxation rates were related to the distribution of the electric field, which was determined using MREIT. Fig. 2A shows an example of subtracted T_2-weighted images obtained as (T_2 map after PEF treatment) - (T_2 map before PEF treatment) of apple, potato, and chicken. The T_2 changes and electric field distribution were evaluated considering a region crossing the centre of the sample. Fig. 2C shows a general decrease in T_2 relaxation times after PEF treatment in both potato and apple tissues, while no significant changes were observed in chicken skeletal muscle exposed to the high voltage pulses.

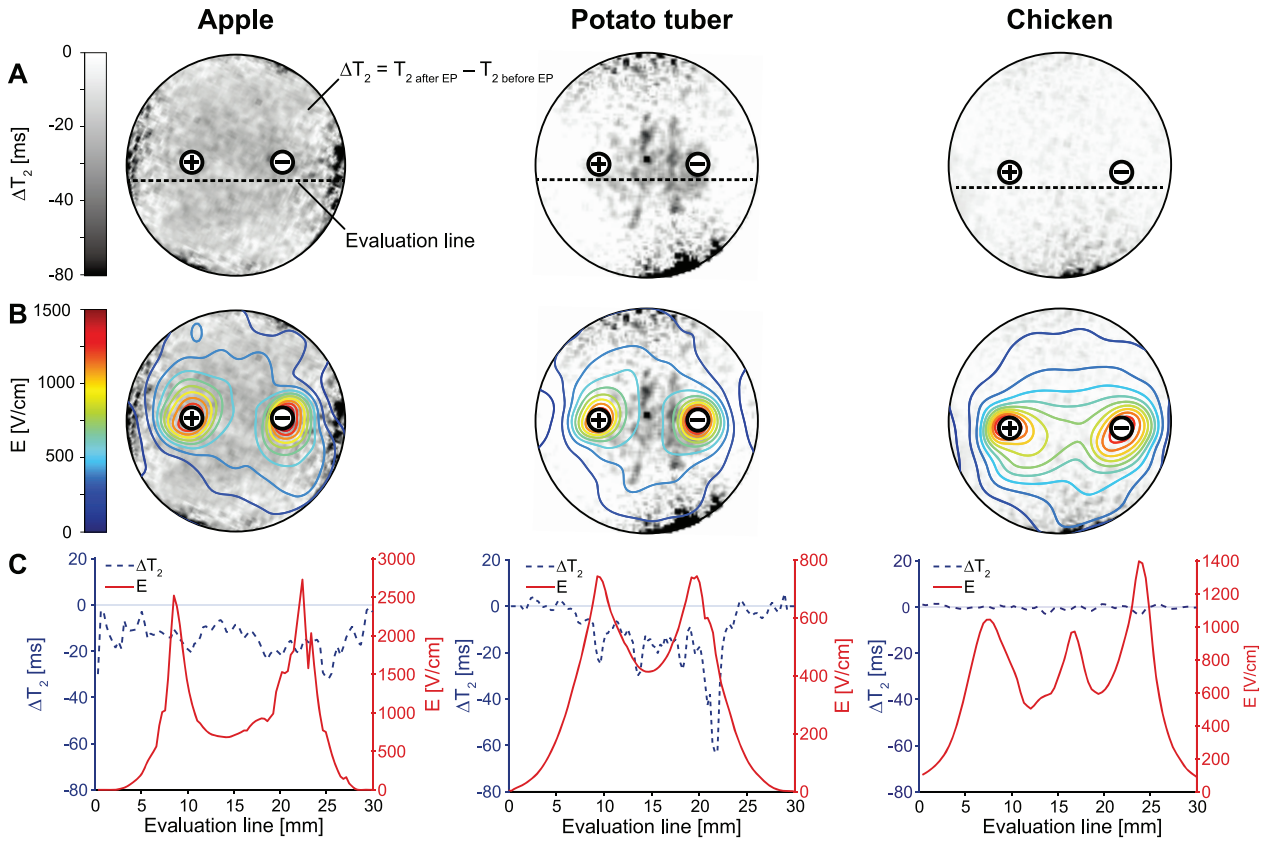

Figure 2. (A) Subtraction of T_2-weighted images acquired before and after electroporation treatment (i.e. total imaging time 18 min after the PEF treatment) in apple tissue, potato tuber and chicken breast. Location of electrodes are marked with + and – sign, while an evaluation line is depicted as black dotted line. (B) The distribution of electric field obtained with MREIT during the electroporation treatment superimposed on the T_2 differences. (C) T_2 differences (blue dotted line) and electric field (solid red line) along the evaluation line.

4. Discussion

Magnetic resonance imaging has been used to monitor spatially-dependent electroporation achieved by PEF treatment in plant tissues [6,10]. Current density imaging (CDI) and magnetic resonance electrical impedance tomography (MREIT) have already been proposed as efficient methods to monitor the electric field distribution in the tissue during the electroporation treatment of plants [6], and for medical applications of electroporation *in vivo*, such as monitoring of the electric field distribution during electroporation of mouse tumours for prediction of reversible [11] and irreversible electroporated areas [12]. In this study, we compared the distribution of the electric field with the transverse relaxation time T_2, which was used as an indicator of the redistribution of water and solutes in the tissues after PEF treatment [13]. In fact, the T_2 relaxation value correlates with the proton exchange between water and solutes, as well as with the diffusion of water protons through internally generated magnetic field gradients, leading to differences in the magnetic

susceptibility of the tissue exposed to the magnetic field, e.g. at the interfaces between air and fluid-filled pores. Therefore, the T_2 values are to some extent associated with the structure of the sample based on its water content. The overall decrease in T_2 in plant tissues due to electroporation could be attributed to the loss of compartmentalisation and diffusion of intracellular water and leakage of ions through the tonoplast and plasma membrane, leading to changes in internal morphology (e.g. shrinkage of total volume) and different water-solution interactions. The ability of MREIT to monitor local changes due to electroporation is most evident in potato tissue, where T_2 changes are only visible in areas exceeding the threshold for electroporation (≈ 250 V/cm for potato). In contrast, no changes in water mobility were detected in chicken breast muscles using MR imaging. Since poultry muscles are composed mainly of fast-twitch fibres associated with anaerobic glycolysis, *rigour mortis* sets in very fast [14]. As rigour progresses, the space in which water can be held in the myofibrils decreases and fluid can be forced into the extra myofibrillar spaces where it is more easily lost as a drip. The absence of T_2 changes in this case study therefore reinforces the premise that the structural layers of the skeletal muscle studied were already severely degraded approximately 48 hours *post mortem,* and therefore no release of intracellular water could be detected by MRI.

5. Conclusions

The monitoring of the electric field distribution during the application of electric pulses using magnetic resonance and electrical impedance tomography is described and experimentally investigated on various complex structures. The research findings provided useful insights into the evaluation of electroporation and suggest that magnetic resonance electrical impedance tomography could be used as an efficient tool to improve the effectiveness of PEF treatment. Since monitoring is performed during pulse delivery, the determined electric field distribution considers all heterogeneities and changes that occur in the treated tissue. This near-real-time information can also be used for fine adjustments of PEF treatment parameters, such as the amplitude of electric pulses, or changing their number during the PEF treatment. Additional research is warranted to cover the full spectrum of possibilities offered by the MREIT in the field of electroporation.

Acknowledgments

This work was supported by the Slovenian Research Agency (research core funding No. P2-0249, funding for Junior Researcher to MS and project No. J2-1733 to MK).

References

[1] Mahnič-Kalamiza S, Vorobiev E and Miklavčič D 2014 Electroporation in Food Processing and Biorefinery *J. Membr. Biol.* **247** 1279–304

[2] Barba F J, Parniakov O, Pereira S A, Wiktor A, Grimi N, Boussetta N, Saraiva J A, Raso J, Martin-Belloso O, Witrowa-Rajchert D, Lebovka N and Vorobiev E 2015 Current applications and new opportunities for the use of pulsed electric fields in food science and industry *Food Res. Int.* **77** 773–98

[3] Langus J, Kranjc M, Kos B, Šuštar T and Miklavčič D 2016 Dynamic finite-element model for efficient modelling of electric currents in electroporated tissue *Sci. Rep.* **6** 26409

[4] Genovese J, Kranjc M, Serša I, Petracci M, Rocculi P, Miklavčič D and Mahnič-Kalamiza S 2021 PEF-treated plant and animal tissues: Insights by approaching with different electroporation assessment methods *Innov. Food Sci. Emerg. Technol.* **74** 102872

[5] Verdiglione R and Cassandro M 2013 Characterization of muscle fiber type in the pectoralis major muscle of slow-growing local and commercial chicken strains *Poult. Sci.* **92** 2433–7

[6] Kranjc M, Bajd F, Serša I, de Boevere M and Miklavčič D 2016 Electric field distribution in relation to cell membrane electroporation in potato tuber tissue studied by magnetic resonance techniques *Innov. Food Sci. Emerg. Technol.* **37** 384–90

[7] Joy M, Scott G and Henkelman M 1989 In vivo Detection of Applied Electric Currents by Magnetic-Resonance Imaging *Magn. Reson. Imaging* **7** 89–94

[8] Khang H S, Lee B Il, Oh S H, Woo E J, Lee S Y, Cho M H, Kwon O, Yoon J R and Seo J K 2002 J-substitution algorithm in magnetic resonance electrical impedance tomography (MREIT): phantom experiments for static resistivity images. *IEEE Trans. Med. Imaging* **21** 695–702

[9] Sersa I 2008 Auxiliary phase encoding in multi spin-echo sequences: application to rapid current density imaging. *J. Magn. Reson.* **190** 86–94

[10] Dellarosa N, Ragni L, Laghi L, Tylewicz U, Rocculi P and Dalla Rosa M 2016 Time domain nuclear magnetic resonance to monitor mass transfer mechanisms in apple tissue promoted by osmotic dehydration combined with pulsed electric fields *Innov. Food Sci. Emerg. Technol.* **37** 345–51

[11] Kranjc M, Markelc B, Bajd F, Čemažar M, Serša I, Blagus T and Miklavčič D 2015 In Situ Monitoring of Electric Field Distribution in Mouse Tumor during Electroporation. *Radiology* **274** 115–23

[12] Kranjc M, Kranjc S, Bajd F, Serša G, Serša I and Miklavčič D 2017 Predicting irreversible electroporation-induced tissue damage by means of magnetic resonance electrical impedance tomography. *Sci. Rep.* **7** 10323

[13] Hjouj M and Rubinsky B 2010 Magnetic resonance imaging characteristics of nonthermal irreversible electroporation in vegetable tissue. *J. Membr. Biol.* **236** 137–46

[14] Schreurs F J G 2000 Post-mortem changes in chicken muscle *Worlds. Poult. Sci. J.* **56** 319–46